Influence of ion irradiation on the structure and mechanical properties of extruded V95 alloy profiles after artificial aging

Influence of ion irradiation on the structure and mechanical properties of extruded V95 alloy profiles after artificial aging

N V Gushchina[1], V V Ovchinnikov[1,2], F F Makhin'ko[1], L I Kaigorodova[3] and S M Mozharovsky[1]

[1] Institute of Electrophysics UD RAS, 106 Amundsen Str., Yekaterinburg, 620016, Russia
[2] Ural Federal Technical University named after the First President of Russia B.E. Yeltsin, 19 Mira Str., Yekaterinburg, 620002, Russia
[3] Mikheev Institute of Metal Physics UB RAS, 18 S. Kovalevskaya Str., Yekaterinburg, 620990, Russia

E-mail: guscha@rambler.ru

Abstract. The effect of 10-keV Ar^+ ion irradiation on the mechanical properties and structural and phase state of hot-pressed thin profiles 1.5 mm thick and made of an V95 alloy (Al-Zn-Mg-Cu system) after artificial aging (T = 140°C, 16 h) has been studied. Ion beam treatment of the alloy (j = 300 μA·cm^{-2}, $F = 1.9 \cdot 10^{15}$ and $1.1 \cdot 10^{16}$ cm^{-2}) without heating the samples to significant temperatures (T < 35–50°C) has not been established to change the ultimate strength and yield strength; however, it increases the relative elongation by 1–2 %. Transmission electron microscopy has shown that irradiation changes the grain structure and the morphology of particles of the crystallization origin in the entire volume of quenched and artificially aged V95 alloy samples (1.5 mm thick). The irradiation does not affect the size and the volume fraction of fine strengthening η´- and η-phase particles.

1. Introduction

Technological expansion requires the development of materials with a complex of high properties, in particular, higher strength with sufficient plasticity for aluminum alloys. The resource of standard thermal and thermomechanical treatments used for this purpose is practically exhausted. Therefore, ion beam treatment technique, using dynamic long-range effects [1, 2] and modifying large-thickness commercial sheets and profiles, may turn out to be promising for the search for new opportunities to improve the properties of aluminum alloys used in the nuclear industry and aerospace engineering.

It has been established that the treatment with 20–40 keV Ar^+ ions leads to increase in the plasticity of cold-worked AMg6, VD1, 1441, 1424 aluminum alloys due to accelerated (compared to conventional annealing) polygonization and recrystallization processes [3–5]. Analysis of data obtained allows to scientists to propose a short-time (from several seconds to tens of seconds) treatment of commercial Al-Mg, Al-Li-Cu-Mg, and Al-Cu-Mg-Mn aluminum alloys with accelerated Ar^+ ion beams (radiation annealing), instead of prolonged (for 0.5−2 h) intermediate high-temperature (320−400 °C) furnace annealing used for cold working of these alloys [6]. This technique can improve the structure of sheet steel by dissolving the coarse intermetallic inclusions of crystallization origin, exclude the transportation of rolls (packages) of sheet metal in thermal furnaces (and return

transportation) from the technology of cold rolling, reduce the annealing time by 1–2 orders of the magnitude to remove cold-worked state and recover plasticity, and decrease the energy consumption of the process by a factor of 2–3.

In addition to replacing the intermediate annealing, to study the possibilities of accelerated ion beam treatment for improving the mechanical properties and the structure of aluminum alloys at final treatment stages is of interest.

Therefore, the aim of this work is to investigate the effect of Ar^+ ion irradiation on the mechanical properties and the structural and phase state of hot-pressed thin V95 alloy (Al-Zn-Mg-Cu system) profiles 1.5 mm thick in the as-delivered state, namely, after quenching and artificial aging (T = 140°C, 16 h).

2. Experimental part

The objects studied in this work were V95 alloy samples 20 cm long, which were cut from extruded profiles PR-101-50 offered by OAO Kamensk-Ural'skii Metallurgical Works. V95 is a high-strength heat hardenable alloy aluminum with zinc, magnesium, and copper. It is used for highly loaded structures operating under high compression pressure [7]. Table 1 lists the alloy composition of the profiles.

Table 1. Chemical composition of profiles made of V95 alloy

Content of elements (wt.%)									
Al	Si	Fe	Cu	Mn	Mg	Cr	Zn	Ti	Ni
balance	< 0.1	0.1	1.6	0.32	2.1	0.13	6.1	0.03	< 0.1

The image and sectional drawing of the profiles are shown in figure 1 and their standard sizes are indicated in table 2. The samples for mechanical tests and the samples for electron microscopy examination (in the initial state and after irradiation) were cut from a bar 1.5 thick. Profiles after quenching and artificial aging (140 °C, 16 h) were subjected to irradiation.

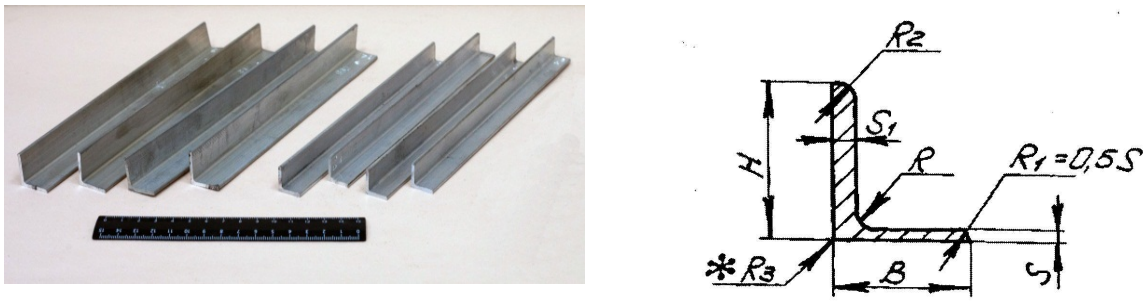

a) b)

Figure 1. Images of (a) V95 alloy profiles and (b) cross section of PR101-50 profiles.

Table 2. Sizes of extruded PR101-50 profiles

Diameter of a circumscribed circle (mm)	Profile size (mm)								Cross-section area (cm^2)
	H	B	S	S_1	R	R_1	R_2	R_3	
25	20	15	1.2	1.5	2	0.6	0.75	0.2	0.468

Irradiation of samples with continuous Ar^+ ion beams was performed in an ILM-1 setup equipped with a PULSAR-1M ion source based on a low-pressure glow discharge with a hollow cold cathode [8]. Samples during irradiation were suspended (from the corners) to prevent their uneven heating. A line-focus ion beam 100 mm×20 mm in cross section was cut from a cylindrical ion beam using a collimator. Samples during irradiation were moved relative to the line-focus beam at a speed of 2 $cm \cdot s^{-1}$. The sample temperature was continuously controlled with the help of a chromel-alumel thermocouple welded to an identical test sample. The ion energy was 10 keV, ion current density was 300 $\mu A \cdot cm^{-2}$, and ion fluence was $1.9 \cdot 10^{15}$ and $1.1 \cdot 10^{16}$ cm^{-2}. The heating temperature of the samples did not exceed 50°C at a maximum fluence.

The static tests for uniaxial tension were conducted at room temperature, according to the standard technique (State Standard GOST 1497-84). The measurement error was ~ 5%. Electron microscopy analysis was carried out by the method of thin foils using a JEM-200 CX transmission electron microscope, at the Electron Microscopy Center of Collaborative Access of the Institute of Metal Physics, UB RAS. Thin foils were prepared from the sections which were parallel to the irradiated surface, at a distance of about 150 μm from irradiated and nonirradiated sides.

3. Details of exposure, measurements and results

Table 3 presents mechanical properties of extruded V95 alloy profiles, which were measured in the initial state and after irradiation.

Table 3 suggests that the ion beam treatment of the alloy under used irradiation conditions (without heating the samples to significant temperatures ($T \sim 35$–50°C) does not change the ultimate strength and yield strength within the measuring error; however, it increases the relative elongation by 1–2%.

Table 3. Mechanical properties of samples in the initial state (after aging) and after irradiation with continuous Ar^+ ion beams

No.	Treatment					Mechanical properties		
						σ_u (MPa)	$\sigma_{0.2}$ (MPa)	δ (%)
1	Quenching and aging (140°C, 16 h)					644	590	11.5
	Ar^+ ion irradiation at the following parameters:							
	E (keV)	j ($\mu A \cdot cm^{-2}$)	F (cm^{-2})	t (s)	T_{ir} (°C*)			
2	10	300	$1.9 \cdot 10^{15}$	1	35	660	600	13.0
3	10	300	$1.1 \cdot 10^{16}$	6	50	633	578	13.6

*The maximum temperature to which a sample was continuously heated under irradiation during the indicated time (without holding at this temperature).

The electron microscopic examination of the V95 alloy microstructure in the initial state after artificial aging (140°C, 16 h) exhibited a fine-grained structure consisting of grains (subgrains) 5–10 μm long and 1–2 μm wide and elongated in the direction of deformation (close to $<112>_{Al}$) (figures 2a, 2b). Figures 2a, 2b show dense dislocation pileups in the grains. In addition, there are extended lath-shaped particles 0.2–0.4 μm long and equiaxed fine precipitations ~ 10–15 nm in diameter (figure 2c). Analysis of lattice distances calculated for additional reflections in electron diffraction patterns (figure 2c) showed that detected lath-shaped particles are mainly Al_6Mn-phase intermetallic compounds. The manganese-bearing phase is also known from the literature to contain Cu and Fe atoms and acquires the composition (Cu, Fe, Mn) Al_6 in Al-Cu-Mg-Zn alloys with iron impurities [9]. In addition, some electron diffraction patterns exhibit the reflections of phase $Al_{18}Cr_2Mg_3$ was detected. The morphology of $Al_{18}Cr_2Mg_3$ and (Cu, Fe, Mn) Al_6 particles is almost the same, according to [10], where the V95 alloy with the same content of impurity elements has been studied. Particles of both intermetallic phases precipitated during the crystallization of the alloy.

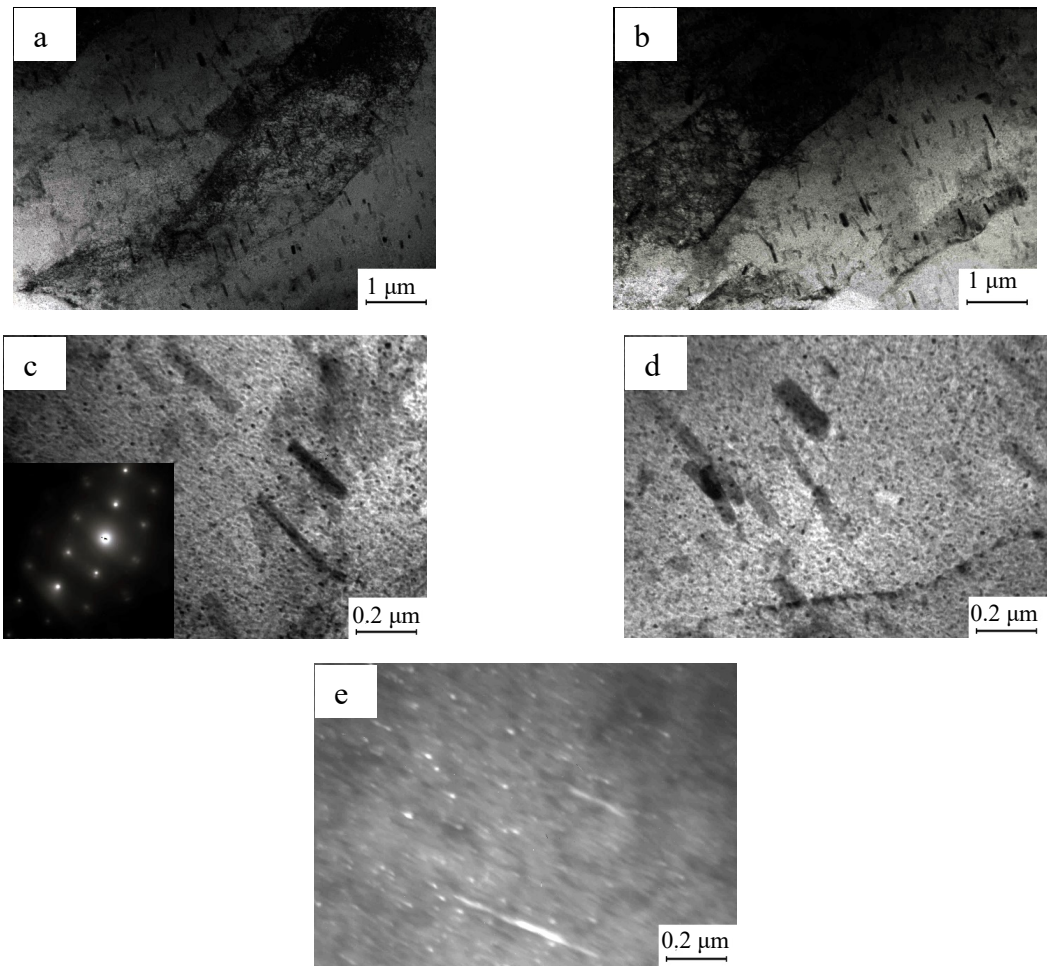

Figure 2. Microstructure of alloy V95 after quenching and artificial aging (140°C, 16 h): (a–d) bright-field images, (a) electron diffraction pattern, zone axis $[110]_{Al}$, and (e) dark-field image in reflections $(310)_{(Cu,Fe,Mn)Al_6} + (103)_{\eta'} + (103)_{\eta}$.

Hardening phases with a hexagonal crystal lattice, namely, metastable η′ and stable η ($MgZn_2$) phases precipitate in the alloy during aging. The particle diameter is 10–15 nm (figures 2c, 2d). The electron diffraction pattern (figure 2c) illustrates weak and blurred reflections. The fraction of each phase after aging under these conditions cannot be identified, since these phases have close lattice parameters and their reflections overlap with each other in the electron diffraction patterns. Analysis of dark-field images in these reflections supported the fact that η′- and η-phase particles are fine (figure 2e). There are also intermetallic compounds (Cu, Fe, Mn) Al_6 in addition to η′- and η-phase particles in the figures.

Figures 2c, 2d demonstrate the particle distribution for both phases over the grain volume and near boundaries. It is seen that the coarse particles of the η phase are uniformly distributed in the bulk of the grains, but their density is negligible (figure 2c). The η phase forms either continuous films of precipitations (figure 2d) or chains of closely located laths along grain boundaries.

In contrast to the stable η phase, the density of fine metastable η′-phase particles well observed in figures 2c, 2d is very high. It should be noted that analysis of the distribution of particles of both phases along grain boundaries has revealed no precipitation-free zones near them, which is one of the main reasons for the decreased plasticity of these alloys (figure 2d).

Analysis of the samples irradiated with argon ions at a fluence of $1.1 \cdot 10^{16}$ cm^{-2} has showed that ion beam treatment affects the structural state of the aged alloy, namely, its grain structure and the morphology of the particles of crystallization origin. No elongated deformation-induced subgrains are observed in the alloy after irradiation (at a distance of 150 μm from the irradiated surface). Subgrains acquire an equiaxed shape. There are dislocation tangles inside the grains (figures 3a, 3b). Some grains are divided into fragments 1–2 μm in diameter (figure 3b). Fragment boundaries are poorly observed, which confirms their low-angle misorientation. However, equiaxed subgrains with well-formed boundaries and of the same size as the fragments (figure 3c) have formed in some regions of the sample.

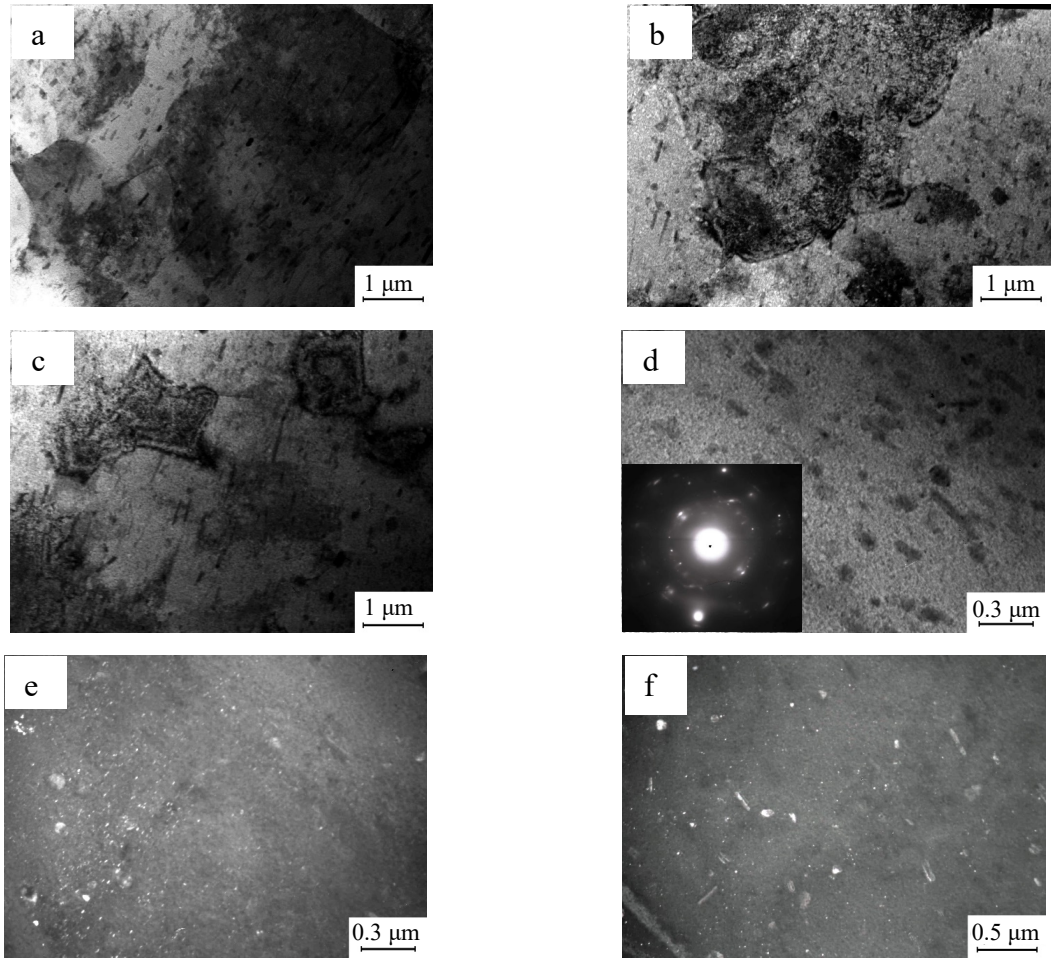

Figure 3. Microstructure of alloy V95 after quenching, aging (140°C, 16 h), and irradiation at a fluence of $1.1 \cdot 10^{16}$ cm^{-2} (near the irradiated surface): (a–d) bright-field images, (e), (f) dark-field images in reflections: (e) $(112)_{\eta'} + (131)_{(Cu,Fe,Mn)Al_6}$ and (f) $(103)_{\eta} + (221)_{(Cu,Fe,Mn)Al_6}$.

The study of the fine structure in the volume of grains showed that irradiation did not affect the phase composition of the aged alloy. The electron diffraction patterns retained clear and pronounced reflections of the intermetallic phase (Cu, Fe, Mn) Al_6 and blurred weak reflections of the hardening η′- and η-phases (figure 3d).

Analysis of bright-field and dark-field images of intermetallic compounds (Cu, Fe, Mn) Al_6 has revealed irradiation-induced changes in their morphology. Thus, the distribution density and the length of lath-shaped intermetallics decrease. The length of laths in the irradiated sample is less than 0.2 μm, and the number of equiaxed particles (~ 50–70 nm in diameter) of this phase has increased (figure 3d).

The dark-field images of these particle are shown in figures 3e, 3f. There are also dark-field images of η′- and η-phases in these figures. The particles of these phases retain their small size after irradiation.

The alloy structure near the unirradiated side of the samples is almost the same that near the irradiated side. Thus, grains elongated in the direction of deformation completely disappeared and an equiaxed grain structure with a grain size of 5–10 μm formed. Fragments of these grains are shown in figures 4a, 4b. A cellular structure inside the grains is poorly seen in the figures, since cell boundaries are decorated with precipitated particles. Equiaxed subgrains about 1 μm in diameter are observed only in separate regions of the sample (figure 4b).

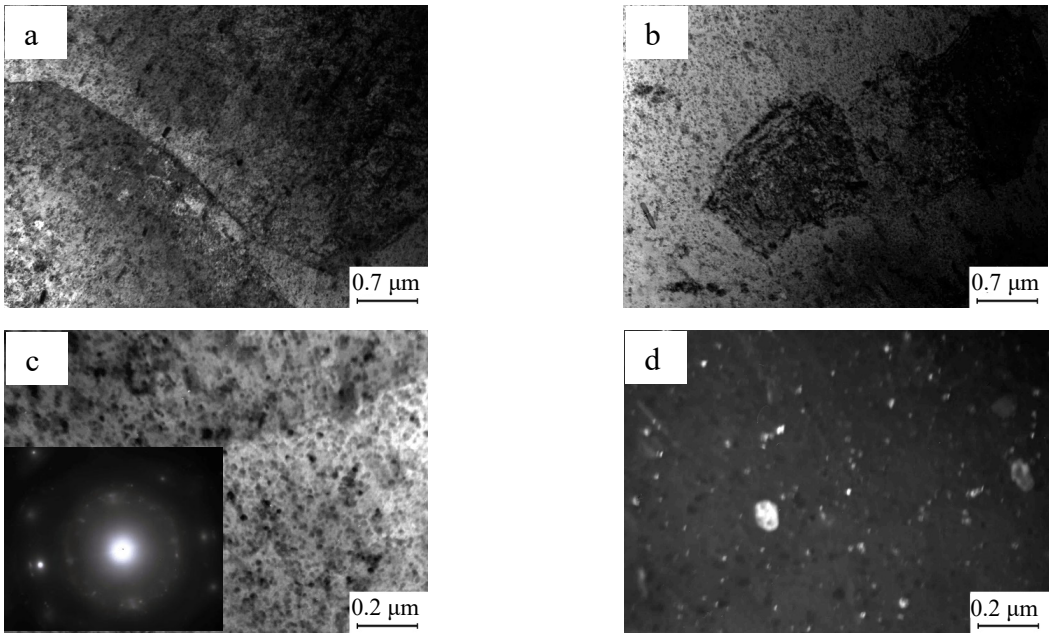

Figure 4. Microstructure of alloy V95 after quenching, aging (140°C, 16 h), and irradiation at a fluence of $1.9 \cdot 10^{16}$ cm^{-2} (near the irradiated surface): (a–c) bright-field images, (c) electron diffraction pattern, zone axis <112>$_{Al}$, and (d) dark-field image in reflections $(103)_{\eta} + (221)_{(Cu,Fe,Mn)Al_6}$.

The examination of the phase composition of the irradiated alloy using additional reflections in electron diffraction patterns showed intermetallic phase (Cu, Fe, Mn) Al_6 and phases η′ and η (figure 4c). As well as near the irradiated surface, of the equiaxed (Cu, Fe, Mn) Al_6-phase particles formed and the particle size of this lath-shaped phase decreased to 0.1–0.2 μm, but individual particles to 0.4 μm in length were retained. Figure 4c shows the bright-field image at a greater magnification. It is seen that the observed phases are uniformly distributed over the grain volume. Figure 4d show the dark-field images of the particles of all phases.

4. Conclusion

The effect of 10-keV Ar^+ ion irradiation on the mechanical properties and structural and phase state of hot-pressed thin profiles (1.5 mm thick) made of an V95 alloy (Al-Zn-Mg-Cu system) after artificial aging (T = 140°C, 16 h) was studied.

It was not established that ion beam treatment of the alloy (j = 300 μA·cm^{-2}, $F = 1.9 \cdot 10^{15}$ cm^{-2} and $1.1 \cdot 10^{16}$ cm^{-2}) without heating the samples to significant temperatures ($T \sim$ 35–50°C) changed the ultimate strength and yield strength; but it increased the relative elongation by 1–2%. This result is interesting, since the improvement of plastic properties while maintaining strength can favorably affect the resource characteristics.

Transmission electron microscopy showed that irradiation changed the grain structure in the entire volume of quenched and artificially aged V95 alloy samples: subgrains lost their elongated shape and

became equiaxed. In addition, irradiation transformed the forms of crystallization-induced (Cu, Fe, Mn) Al_6 intermetallic compounds. This manifested in less extended laths to 0.1–0.2 μm and the increased number of equiaxed particles ~ 50–70 nm in diameter. The irradiation under the above conditions did not affect the size and the volume fraction of fine strengthening η′- and η-phase particles.

Acknowledgments
This work was supported in part by RFBR (grant No. 19-08-00802-a).

References
[1] Ovchinnikov V V 2008 *Phys. Usp*. **51** 955
[2] Ovchinnikov V V 2018 *Surface and Coating Technology* **355** 65
[3] Ovchinnikov V V, Gavrilov N V, Gushchina N V *et al* 2010 *Russian metallurgy (Metally)* **3** 2007
[4] Ovchinnikov V V, Mozharovsky S M, Gushchina N V, Makhinko F F, Kaigorodova L I, Kolobnev N I and Hohlatova L B 2014 *Izv. Vyssh. Uchebn. Zaved. Fiz.* **57** 206 [in Russian]
[5] Ovchinnikov V V, Gushchina N V, Mozharovsky S M and Kaigorodova L I 2017 *IOP Conference Series: Materials Science and Engineering* **168** 012067
[6] Ovchinnikov V V, Gavrilov N V, Gushchina N V *et al* 2009 *Method of production of aluminum sheets* RF Patent no. 2363755 Byull. Izobr. 22 [in Russian]
[7] Kolachev B A, Elagin V I and Livanov V A 2001 *Metalloved. Term. Obrab. Zvet. Met Splav* (MISiS, Moscow, 2014)
[8] Gavrilov N V, Mesyats G A, Nikulin S P, Radkovskii G V, Eklind A and Perry A J 1996 *J. Vac. Sci. Technol. A* **14** 1050
[9] Mondol'fo L F 1979 *Structure and Properties of Aluminum Alloys* (Moscow: Metallurgiya) [in Russian]
[10] Kaigorodova L I, Zamyatin V M and Popov V I 2005 *Physics of Metals and Metallography* **99** 75